

The crystallization kinetics of polyethylene under isothermal and non-isothermal conditions

S. Chew, J. R. Griffiths and Z. H. Stachurski*

Department of Materials Engineering, Monash University, Melbourne, Australia 3168
(Received 27 July 1988; accepted 18 November 1988)

The work presented here is concerned with relationships between isothermal and non-isothermal crystallization kinetics in high-density polyethylene. First, information on the nucleation, growth and transformation rates during isothermal crystallization is presented and a time-temperature-transformation diagram is produced. Secondly, the results of simulating continuous cooling thermal treatments by a series of stepped isothermal experiments are reported. Finally, the non-isothermal data are analysed in terms of the isothermal properties, using a linear additivity rule. All the observations were made on a hot-stage optical microscope: the limitation that this technique places on the observation of small nuclei is commented on.

(Keywords: high-density polyethylene; crystallization; thermal history; time-temperature-transformation diagram; additivity)

INTRODUCTION

Polymers are invariably processed under continuous cooling (non-isothermal) conditions so that an ability to predict the crystallization kinetics under such conditions is of enormous practical significance. Two approaches to the problem can be taken. First, a purely empirical solution can be obtained by simply measuring crystallization rates at various cooling rates—both constant and otherwise. Indeed, this solution is widely adopted by metallurgical industries, for example, those concerned with the heat treatment of steel: an 'atlas' of 'continuous cooling transformation' (CCT) diagrams is available for various grades of steel, heat-treated under various cooling rates. However, this approach has its shortcomings. Thus, even the most exhaustive set of experiments cannot include all conceivable thermal histories so that interpolation is necessary. Furthermore, the consequences in the polymer processing field of, for example, varying the nucleation rate with additives are not easily included. Such shortcomings have stimulated a search for a predictive method which can account for effects such as those described above. The simplest of these methods is based on the measured isothermal crystallization rates. Such isothermal crystallization can often be described by the 'Avrami equation'^{1,2}:

$$X(t, T) = 1 - \exp[-K(T)t^{m(T)}] \quad (1)$$

in which X is the volume fraction of crystalline material at a time t and at a constant temperature T , and in which K usually varies strongly, and m weakly, with T . Many attempts³⁻¹⁰ have been made to derive non-isothermal crystallization rates from equation (1). All have been

based on an 'additivity' principle that:

$$\int_0^\tau \frac{d\tau}{t_a(T)} = 1 \quad (2)$$

in which τ is the time in the non-isothermal reaction to reach a certain value of X (denoted by X_a) and $t_a(T)$ is the time at constant temperature T for the same value of $X = X_a$. However, it is well known that equations (1) and (2) can only be combined if certain restrictions are met; for example, the rate of crystallization at any temperature is independent of the prior thermal history¹⁻⁴. At present, the additivity rule has been applied only to solid \rightarrow solid transformations in metal alloys, notably in steel^{9,10}. Such transformations are particularly complex and it is unlikely that the necessary restrictions apply. This is recognized by the descriptions of additivity as 'a well established empirical rule'¹¹ and its application as requiring 'theory and some empirical inputs'¹². Problem areas typical of solid-state transformations include: compositional gradients in the transforming alloy; the existence of thermodynamically metastable (or 'intermediate') precipitates; elastic distortions associated with volume changes and interfacial coherency strains.

In the light of these comments the aim of the present study is:

(a) to investigate additivity in a system where the complications alluded to above do not exist (a suitable choice being the crystallization from the liquid state of a pure substance, polyethylene), and

(b) to produce a predictive method of use to the polymer processing industry.

In this paper we report the results of some studies of the additivity rule on a particular grade of high-density polyethylene (HDPE). During crystallization, the temperature is varied in simple steps, and the time to achieve

* To whom correspondence should be addressed

a certain amount of crystallization is measured and compared against that calculated from isothermal experiments.

Since isothermal crystallization provides the data for use with the additivity rule, this paper also includes a complete set of isothermal crystallization results for the polyethylene between the temperatures of 121 and 129°C.

EXPERIMENTAL METHOD

Observations were made of the crystallization of thin films (1–2 μm thick) of molten polyethylene on glass slides using a hot-stage microscope. Photographs were taken periodically and were used to determine the number and size of the crystals (spherulites) during crystallization of the sample. Further details are given below.

Material

The polyethylene sample used in this study was prepared from unfractionated Hostalen GC-6165 HDPE, a non-commercial grade prepared by Hoechst Australia Ltd.

The polymer was purified by precipitation from *o*-dichlorobenzene. The experimental procedure involved dissolving 20 g of HDPE in 1.5 litres of redistilled *o*-dichlorobenzene under reflux (1 h, 180°C). Nitrogen was bubbled through the solvent as it was heated to the boiling point, and during the period of reflux, in order to exclude oxygen from the system. Next, the solution was filtered, transferred into a beaker, and allowed to cool under an atmosphere of nitrogen. When the polymer had precipitated out of the solution, it was filtered off, washed with redistilled acetone and dried under vacuum to constant weight. Gel permeation chromatography showed that $\bar{M}_w = 160\,000$ and $\bar{M}_n = 26\,000$.

Sample preparation

Previous workers^{13–15} have reported that a special 'pretreatment' is necessary in order to produce optically resolvable spherulites in polyethylene. The pretreatment reduces or inactivates a large proportion of the heterogeneous nuclei that exist in the untreated material. The pretreatment technique of filtration with micropore filters suggested by Hoffman *et al.*¹⁵ was tried without success, a result also noted by Maxfield and Mandelkern¹⁶. However, success was achieved with the method of Banks *et al.*¹³. About 10 mg of purified HDPE was sprinkled onto a glass slide preheated to 290°C. A coverslip was pressed onto the molten HDPE drop to minimize oxidation and, at the same time, to obtain a thin-film specimen (estimated to be 1–2 μm thick). After 20 s, the glass slide and sample were removed from the hot stage and allowed to cool in air. Although this procedure resulted in optically resolvable spherulites, the spherulite size (and, therefore, their numbers) was not constant throughout the specimen, the edges tending to have fewer and larger spherulites compared with the centre. In order to achieve consistent results, all the observations reported in this paper were made at one place in the central region.

Apparatus

Observations were made using a Mettler FP-82 hot stage, mounted on a microscope, with heating and cooling being controlled by a Mettler FP-80 unit. Pre-set

temperatures can be kept constant to $\pm 0.1^\circ\text{C}$ and heating or cooling rates of up to $20^\circ\text{C min}^{-1}$ are possible. Visual observations were made at a magnification of $\times 63$, and a 35 mm camera attached to the microscope was used for photographic recording at a magnification on the film of $\times 40$. The microscope was operated in the transmitted-light phase-contrast mode, this being more useful than the polarizing mode for detecting small spherulites. The smallest spherulites that could be detected with confidence had a radius of $\sim 5\ \mu\text{m}$.

Measurement of the growth rate, \dot{G} , and the nucleation rate, \dot{N}

The photographic negatives were projected onto a screen for measuring the radius of spherulites and half-length of axialites. The instantaneous growth rate, \dot{G} , was determined by measuring these quantities at successive times, t :

$$\dot{G} = dR/dt \quad (3)$$

The number and different sizes of spherulites visible on the photographs were determined with the aid of a Carl Zeiss Particle Size Analyser TGZ-3. It is assumed that each spherulite originates from a single nucleus, the critical size of the nucleus being of the order of 10 nm. Nuclei are essentially invisible until they grow to a radius of $\sim 5\ \mu\text{m}$. Nevertheless, it is possible to determine the time when the nucleation event occurs by adopting the method of Aggarwal *et al.*¹⁷. This involves dividing (the radius of each particular spherulite minus the critical nucleus radius) by the measured growth rate: it is assumed that the growth rate is constant from the formation of the nucleus onwards. It is then possible to plot the true number of nuclei as a function of time.

The apparent nucleation rate, \dot{n} , is:

$$\dot{n} = (1/A)(dn/dt) \quad (4)$$

where A is the area of the field of view and n is the number of nuclei*.

The true nucleation rate, \dot{N} , is defined as the nucleation rate per area of untransformed material^{18,19}:

$$\dot{N} = \dot{n}/[1 - X(t, T)] \quad (5)$$

At any time, t , the value of $X(t, T)$ is found by superimposing a square grid of points over the photograph and using a point-counting technique whereby:

$$X(t, T) = P_t/P_0 \quad (6)$$

where P_t is the number of points lying within the spherulites and P_0 is the total number of points.

RESULTS: PRELIMINARY EXPERIMENTS

The sample, prepared as described above, was melted on the hot stage at an initial temperature $T^* > T_m$, held there for a certain time, t^* , and then cooled to a predetermined crystallization temperature, T_c , at a certain cooling rate. Observations were made at T_c until crystallization was complete, where upon the sample was reheated to T^*

* A better definition of nucleation rate would involve the volume of the examined material rather than its area. However, because the film thickness is not well known, we have preferred the area definition; furthermore, since the smallest observable spherulite is already larger than the film thickness, the experiment is in a sense two-dimensional

prior to the next experiment at a new T_c . During the entire set of experiments only the one field of view in the one sample was examined at the various T_c temperatures. This preliminary set of experiments was done to observe the effects of T^* , t^* and cooling rates on the rate of nucleation at one particular value of T_c ($T_c = 125^\circ\text{C}$). The results are summarized in Figure 1, in which the number of spherulites/mm² is plotted as a function of time. It can be seen that the data fall into two groups. One, in which T^* was low or the holding time t^* was short, had a relatively high number of spherulites ($\sim 600/\text{mm}^2$). The larger number of spherulites in this first group is attributed to incomplete melting of the solid. In the second group, for which $T^* > 140^\circ\text{C}$ and $t^* > 10$ min, the number of spherulites was found to be $\sim 540/\text{mm}^2$. From these tests the growth rate, \dot{G} , was evaluated, and the results are given in Figure 2. It can be seen that \dot{G} is completely unaffected by the variables used in the investigation.

RESULTS: ISOTHERMAL EXPERIMENTS

Based on the information in Figures 1 and 2 the standard initial conditions for the remainder of the research were that the sample, pretreated as described previously, was

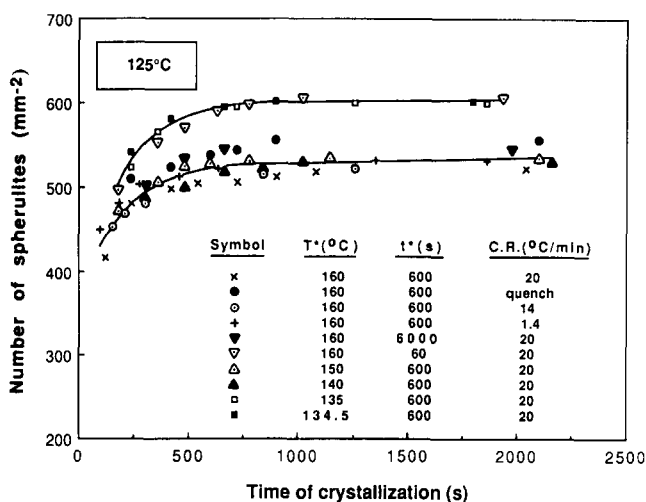


Figure 1 Observed number of spherulites vs. time of crystallization for various temperatures T^* , hold times t^* and cooling rates CR

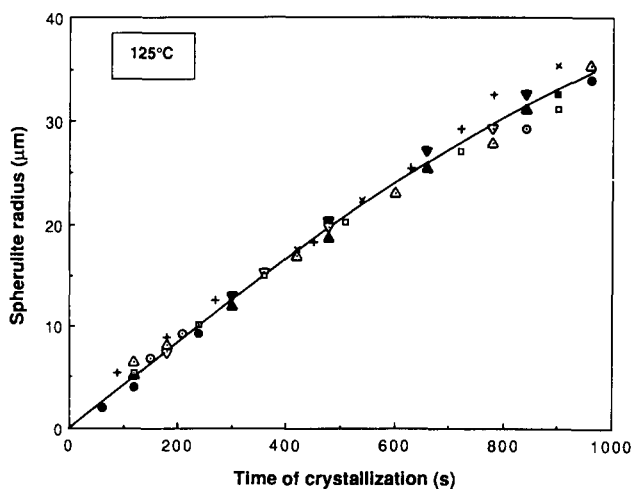


Figure 2 Observed spherulite radius vs. time for various temperatures T^* , hold times t^* and cooling rates CR (for legend to points see Figure 1)

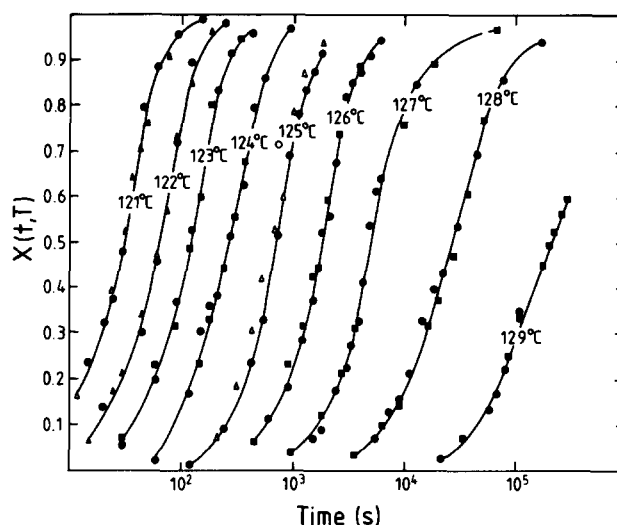


Figure 3 Fraction of transformation $X(t, T)$ vs. time for various crystallization temperatures T_c : (●) first set of measurements; (■) second set of measurements; (▲) third set of measurements after completion of non-isothermal tests

Table 1 Results of isothermal experiments^a

T_c ($^\circ\text{C}$)	$t_{0.5}$ (s)	\dot{G} (nm s^{-1})	n (mm^{-2})
121	30.5 ± 3.5	523 ± 135	577
122	65 ± 5	245 ± 58	545
123	115 ± 10	142 ± 17	524
124	250 ± 20	77 ± 7.5	465
125	650 ± 70	41.5 ± 4.5	282
126	1800 ± 200	13.7 ± 2.1	481
127	4700 ± 400	5.74 ± 0.6	387
128	$25\,000 \pm 2500$	1.55 ± 0.12	373
129	$195\,000 \pm 25\,000$	0.287 ± 0.005	303

^a The absolute ranges of values found in two or three experiments are also indicated.

heated to a melt temperature $T^* = 160^\circ\text{C}$, held there for 15 min and then cooled at $20^\circ\text{C min}^{-1}$ to various crystallization temperatures T_c . Only values of T_c between 129 and 121°C were studied: at higher temperatures complete crystallization would have taken weeks (which was considered needlessly long) while below 121°C the crystallization rate was too rapid to be followed accurately with our recording methods (see below, Figure 3). As indicated above, these experiments were performed with one sample and at the same position on the hot stage to avoid any variations in crystallization rate which might occur at different positions in the sample.

Crystallization kinetics

Measurements of the crystallization of the sample as a function of time at various T_c are shown in Figure 3. The times, $t_{0.5}$, for half of the material to have crystallized are given in Table 1. The measurements were repeated twice, once immediately following the first set of measurements, and a second time after the completion of the non-isothermal crystallization experiments, which are described later. Thus Figure 3 contains three sets of data superimposed on the same graph. It can be seen that the data are highly reproducible for the range of T_c temperatures studied. There was no evidence for degradation of the sample, except for a brownish stain observed at the

edges of the specimen, well away from the observational area.

The data from Figure 3 can be used to plot an isothermal time-temperature-transformation (TTT) diagram. This limited TTT diagram, given the small range of studied temperatures, is shown in Figure 4, with curves shown for crystallized volume fractions $X(t, T) = 0.1, 0.5$ and 0.9 .

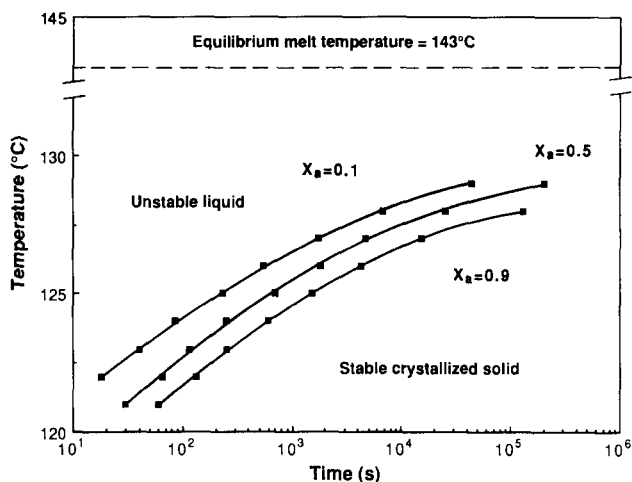


Figure 4 Time-temperature-transformation (TTT) diagram

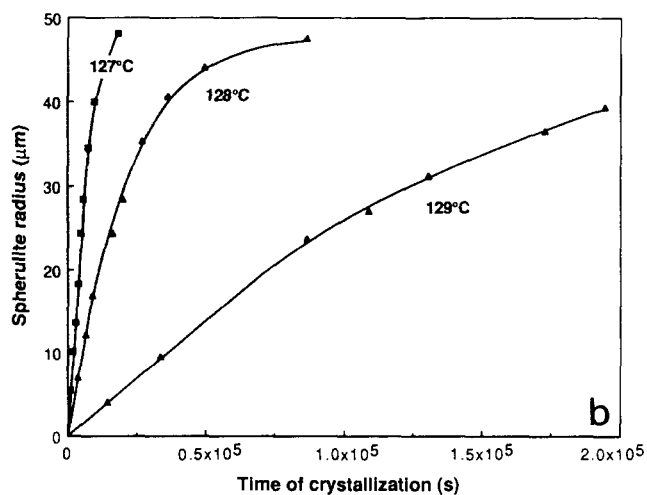
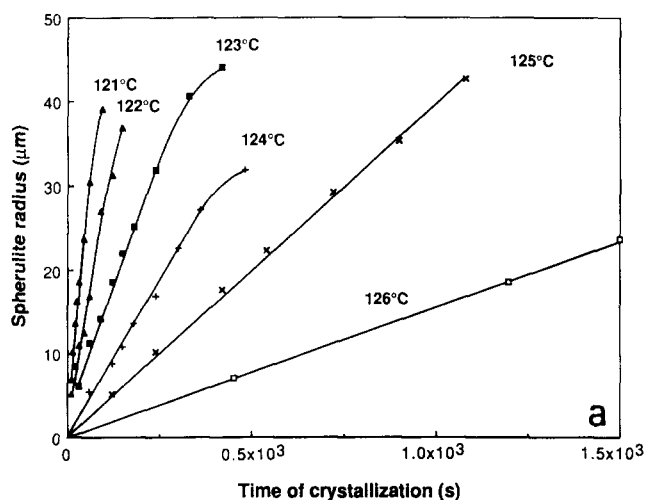


Figure 5 Spherulite size vs. time of crystallization at various T_c

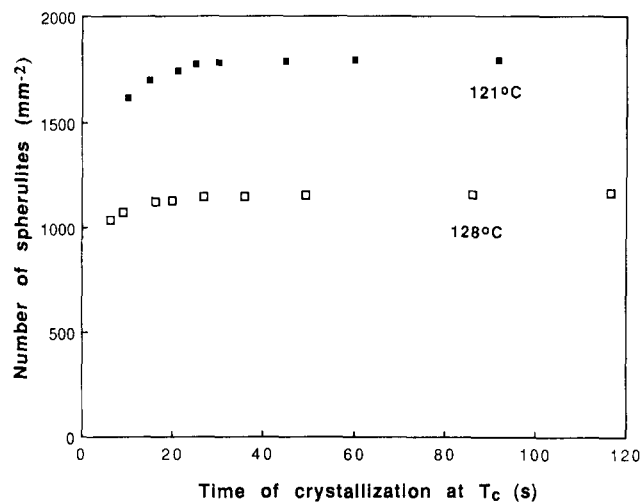


Figure 6 Observed number of spherulites vs. time for $T_c = 121$ and 128°C (times for $T_c = 128^\circ\text{C}$ should be multiplied by 1000)

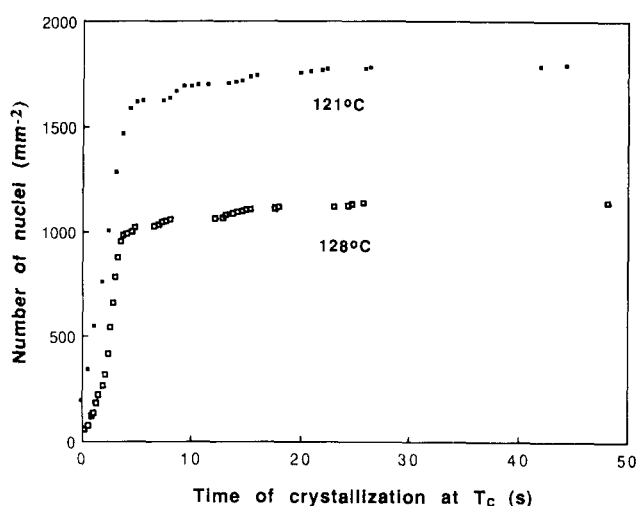


Figure 7 Calculated number of nuclei vs. time of crystallization at $T_c = 121$ and 128°C according to the method of Aggarwal *et al.*¹⁷ (times for $T_c = 128^\circ\text{C}$ should be multiplied by 1000)

Growth kinetics

The growth rates, \dot{G} , were measured on a number of spherulites at each T_c and the results are given in Figure 5 and Table 1. In the initial stages of crystallization, \dot{G} is constant with time, but is very sensitive to T_c . Notice that, at long times ($X \geq 0.65$), \dot{G} decreases significantly. Such behaviour coincides with visible segregation of lower-molar-mass species ahead of the growing front of the spherulites, and has been reported previously^{20,21}.

Nucleation kinetics

The numbers of spherulites on the photographs were counted, divided by the area of the field of view, and plotted at successive times of crystallization. Figure 6 shows data for two selected temperatures: $T_c = 121$ and 128°C . Using the measured sizes of individual spherulites together with the known growth rates, the data can be transformed back in time to the events of nucleation, resulting in a plot of numbers of nuclei versus time as shown in Figure 7. The total number of spherulites in the completely crystallized samples is given in Table 1 for the various crystallization temperatures.

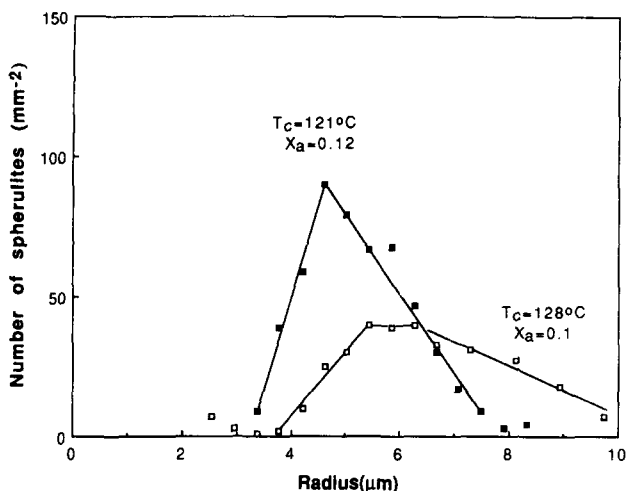


Figure 8 Distribution of spherulite sizes plotted from experimental measurements using Carl Zeiss Particle Size Analyser

In order to ascertain the type of nucleation, the distribution of spherulite sizes (measured using a Carl Zeiss Particle Size Analyser) was plotted for two temperatures, and is shown in Figure 8. These plots correspond to crystallization at a small fraction of transformation, i.e. $X \approx 0.1$. For higher values of X , the measurement of spherulite sizes was unreliable owing to their impingement. The peak character of the plot indicates a heterogeneous type of nucleation: all spherulites are more or less of the same size.

Spherulite morphology

It is a well established fact that spherulite morphology depends strongly on the temperature of crystallization and on the molar mass and its distribution¹⁵. In our studies, the only variable is the temperature of crystallization. Three distinct morphologies were observed within the range of temperature studied, namely (i) round, ringed spherulites at $T_c = 121^\circ\text{C}$, gradually transforming to (ii) coarse, non-ringed spherulites at around $T_c = 126^\circ\text{C}$, leading finally to (iii) axialites for T_c greater than 127°C . These morphologies are illustrated in Figure 9.

RESULTS: NON-ISOTHERMAL EXPERIMENTS

All the data for these experiments were collected on the same sample and in the same field of view as was used for the earlier work. Continuous cooling was modelled by a succession of isothermal transformations at decreasing T_c . Figure 10 shows schematically the thermal history that was applied to the specimen.

Morphological change due to a change in T_c

When crystallization proceeds at T_{c1} and thereafter at T_{c2} , the morphology typical of growth at T_{c1} changes to the morphology typical of growth at T_{c2} . Figure 11 illustrates the transformation of ringed spherulites grown initially at 121°C to coarse-textured spherulites when crystallizing subsequently at 128°C . Conversely, Figure 12 illustrates the development of ringed spherulites at 121°C from an axialite grown initially at 128°C .

Response of the growth rate to a change in T_c

The data in Figure 2 show that \dot{G} is insensitive to the thermal history of the sample—particularly the initial

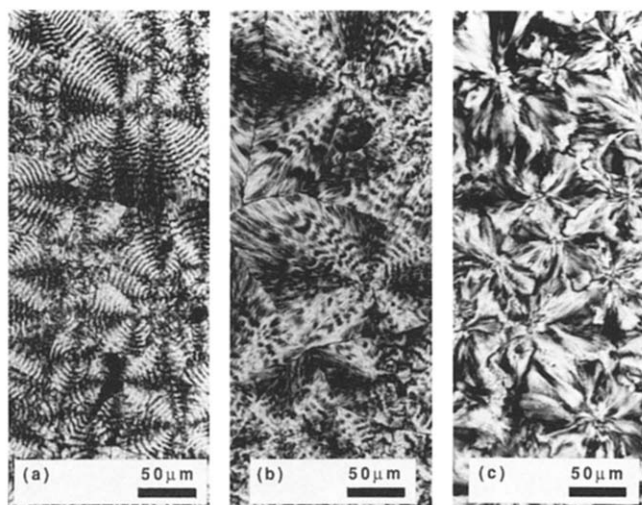


Figure 9 Three morphologies of spherulites observed in polyethylene in this study: (a) ringed spherulites crystallized at 121°C ; (b) coarse-grained spherulites crystallized at 126°C ; and (c) axialites grown at 127°C

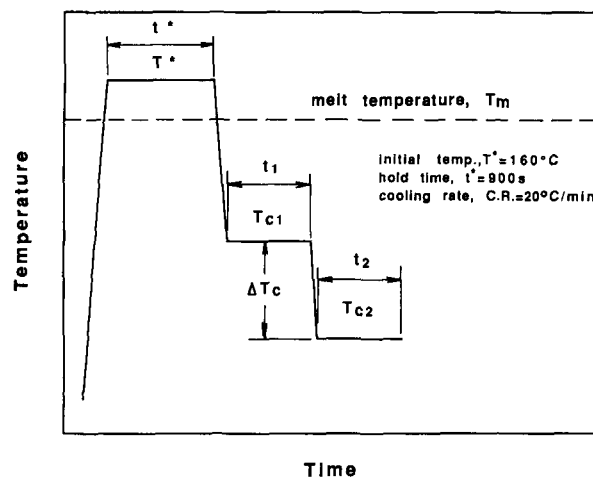


Figure 10 Schematic representation of the thermal history approximating continuous cooling

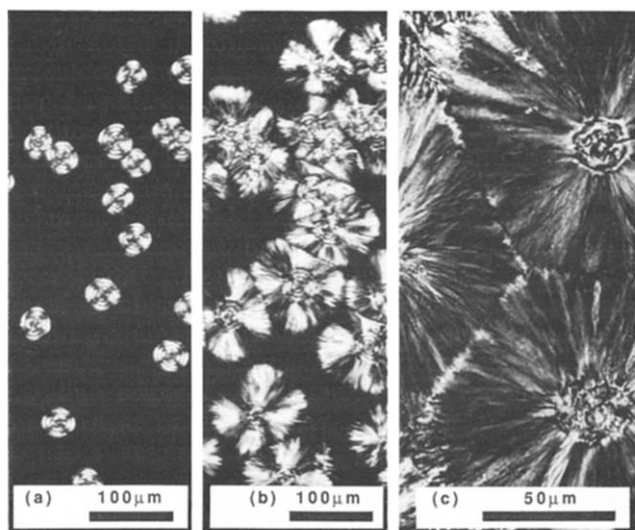


Figure 11 Ringed spherulites undergoing transformation to coarse-grained spherulites: (a) after initial crystallization at 121°C ; (b) subsequent crystallization at 128°C ; and (c) later stage at 128°C . Note that (a) and (b) show the same area

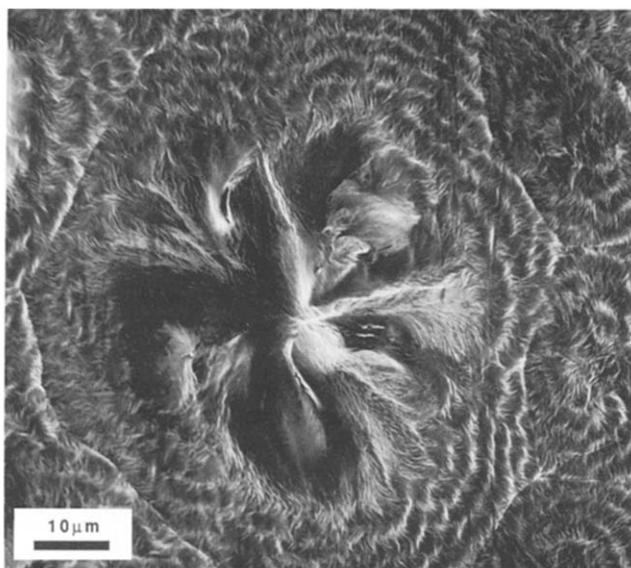


Figure 12 Scanning electron micrograph of an axialite crystallized at 128°C and transformed to a ringed spherulite when cooled and crystallized further at 121°C

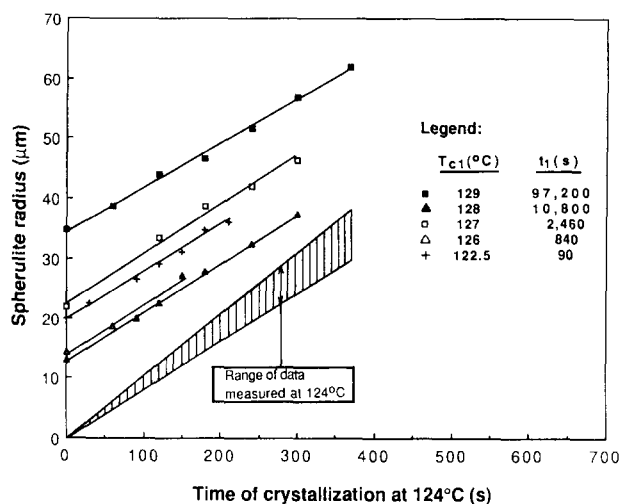


Figure 13 Observed spherulite radius vs. time of isothermal crystallization at 124°C after initial crystallization at various T_{c1} and t_1

melt temperature T^* , the hold time t^* and the cooling rate from T^* to T_c . The results of further experiments to investigate the effect of a partial crystallization at T_{c1} on the subsequent growth rate at T_{c2} are shown in *Figure 13* for the particular case of $T_{c2} = 124^\circ\text{C}$. Also shown in *Figure 13* is the range of growth rates found in several isothermal experiments at 124°C. It is observed that the growth rate, \dot{G} , is not affected by the preceding crystallization history, regardless of whether T_{c1} is greater or less than T_{c2} ; nor is it affected by the initial morphology of the spherulites.

Response of the nucleation behaviour to a change in T_c

When the crystallization temperature is lowered from T_{c1} to T_{c2} a number of nuclei form at T_{c1} and additional nucleation then occurs at T_{c2} . The total number of nuclei formed at T_{c2} might be expected to be less than for an isothermal experiment carried out entirely at T_{c2} . This is because the growing spherulites at T_{c1} will have obliterated some nucleation sites. However, the temper-

ature variation of the nucleation rate is not strong (*Table 1*) and, in fact, we could not determine a difference in the number of nuclei between our non-isothermal and our isothermal experiments. Accordingly, the number of nuclei was essentially independent of the thermal history during crystallization.

Response of the crystallization rate to a change in T_c

Several experiments of the sort indicated in *Figure 10* were done. A typical result is shown in *Figure 14*. The sample was crystallized to about $X = 0.29$ at 128°C before cooling it to 125°C to allow crystallization to be completed. It can be seen that the rate of crystallization at the second temperature is not affected by the prior crystallization, so that the additivity rule should apply.

The results for all the non-isothermal experiments are set out in *Table 2*. The additivity rule summation is given according to the following method. Consider the experiment shown in *Figure 14* (which corresponds to the second experiment tabulated in *Table 2*). We choose an easily observable value for X_a (say, $X_a = 0.5$). In an isothermal experiment at 128°C the time to achieve $X_a = 0.5$ is $t_a = 25 \times 10^3 \pm 2.5 \times 10^3$ s and at 125°C it is 650 ± 70 s (see *Figure 3* and *Table 1*). In the non-isothermal experiment the time at $T_{c1} = 128^\circ\text{C}$ was $t_1 = 14.4 \times 10^3$ s so that the time required at $T_{c2} = 125^\circ\text{C}$ to achieve $X_a = 0.5$ was $t_2 = 255$ s so that $t_2/t_{0.5} = 0.39 \pm 0.05$. Accordingly, the sum $\sum t_i/t_a(T) = 0.97 \pm 0.11$ and the additivity rule applies. The average value for the summation for the 12 experiments given in *Table 2* is 0.99, with a standard deviation of ± 0.05 .

DISCUSSION

Nucleation

The nucleation of spherulites in our experiment is, essentially, heterogeneous. The evidence for this is two-fold. First, it became clear that spherulites would reappear in almost identical positions when the sample had been melted and recrystallized. Secondly, both the nucleation rate measurements (*Figure 7*) and the spherulite size distribution histogram (*Figure 8*) confirm that the

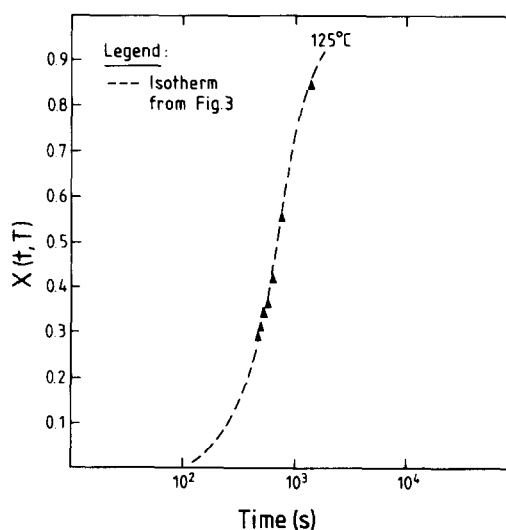


Figure 14 Superposition of two-step isothermal transformation data onto the curve of isothermal transformation: (\blacktriangle) experimental data of $T_{c1} = 128^\circ\text{C}$, $t_1 = 14.4 \times 10^3$ s, $X_1 = 0.29$ and $T_{c2} = 125^\circ\text{C}$

Table 2 Results of non-isothermal experiments^a

T_{c1}	t_1	T_{c2}	t_2	T_{c3}	t_3	T_{c4}	t_4	T_{c5}	t_5	$\Sigma \Delta t/t_n(T)$
(°C)	(10 ³ s)	(°C)	(10 ³ s)	(°C)	(s)	(°C)	(s)	(°C)	(s)	
129	57.6	126	1.11	—	—	—	—	—	—	0.91
128	14.4	125	0.255	—	—	—	—	—	—	0.97
127	2.4	124	0.15	—	—	—	—	—	—	1.11
126	0.66	123	0.066	—	—	—	—	—	—	0.94
129	55.8	127	1.5	125	312	—	—	—	—	1.09
128	5.4	126	0.72	124	90	—	—	—	—	0.98
127	2.4	125	0.195	123	27	—	—	—	—	1.05
129	59.4	127	0.54	125	180	123	30	—	—	0.96
129*	4.2	127	0.90	125	300	123	30	—	—	0.94
128	2.4	126	0.36	124	90	122	18	—	—	0.93
129*	3.6	128*	1.8	127	900	126	450	125	270	0.95
128*	1.8	127*	0.9	126	450	125	90	124	90	1.01

^a The asterisk (*) denotes that the duration at T_c is insufficient for the development and observation of spherulites

majority of nuclei form in the early stages of transformation. (Note that the formation of nuclei at negative times (Figure 7) may mean that they form during the period of cooling from T^* to T_c .) Nevertheless, it is also clear (Figure 7) that, during the early stages of transformation, the numbers of nuclei increase almost linearly with time—that is, nucleation is continuous with time. This early continuous nucleation regime has been observed previously with other polymers^{22–25} and has been described as pseudo-homogeneous nucleation.

According to Hoffman and Lauritzen²⁶, when heterogeneities present in a polymer melt do not interact strongly with the polymer crystal, they are incapable of inducing instantaneous nucleation. The poor wetting of the heterogeneities by the polymer causes some spherulites to appear only after an 'incubation' period. Hence the number of nuclei progressively increases with time until all heterogeneities that are active at a particular temperature are exhausted, nucleation ceases and no further spherulites are observed.

Growth

The constant growth rate of the spherulites observed over most of the transformation period is not unexpected. However, at some later stages of crystallization, a progressively reducing growth rate was recorded. Banks¹³ and Barnes²⁷ reported similar growth characteristics in polyethylene and poly(ethylene oxide), respectively. It is possible to associate the reduced growth rate observed at later stages of crystallization with: (i) the accumulation of non-crystallizable material at the periphery of the spherulite and (ii) the segregation of molecular weights during the crystallization process. Keith and Padden^{20,21} first suggested that 'impurities' of low molecular weight are sufficiently mobile in the melt to diffuse away radially from the advancing spherulites, and cause this effect.

Transformation kinetics

The sensitivity of the crystallization kinetics of HDPE with respect to T_c has already been illustrated in Figure 3. A series of sigmoidal curves was produced when plotting $X(t, T)$ vs. log time. Previous workers^{28,29} have made the observation that individual isotherms can be brought into coincidence simply by shifting each curve by a distance along the time axis. Our results also indicate that superposition of isotherms is possible for the trans-

formations between 121 and 127°C. Superposition has been described by Avrami¹ as being characteristic of 'isokinetic' crystallization and as being a necessary condition for the application of an additivity rule. For crystallization at and above 128°C, the slope of the transformation curves changes and hence superposition is not possible.

As illustrated in Figure 14, the transformation isotherm of the specimen crystallizing isothermally at 125°C after initial crystallization at 128°C can be made to coincide with the transformation isotherm of the specimen crystallized completely at 125°C by merely shifting along the time axis. Indeed, superposition of the transformation isotherms can be achieved regardless of the number of crystallization temperatures in these 'down-quench' experiments.

The additivity rule

The possibility of superposing transformation isotherms along the time axis for a variety of combinations of T_c and ΔT_c suggests that the additivity rule should be applicable when simulating a continuous cooling path with a series of decreasing isothermal crystallizations.

Cahn³ suggested that as long as nucleation sites saturate early during transformation and provided \dot{G} is a function of its instantaneous temperature only, such a state can also be considered as isokinetic. Figure 13 shows that \dot{G} of our HDPE is indeed not influenced by its immediate, previous thermal history but only by the instantaneous transformation temperature.

Cahn has described the condition which is necessary for the application of an additivity rule:

$$n = \text{constant} \quad \dot{G} = \dot{G}(T) \quad (7)$$

where n is the number of nuclei (independent of time and temperature) and \dot{G} is the growth rate (dependent on temperature only). It might be thought that the less restrictive condition:

$$n = n(T) \quad \dot{G} = \dot{G}(T) \quad (8)$$

should also be sufficient, providing that n is independent of thermal history. Our experimental results correspond approximately to this latter condition. We have an early site saturation (see Figures 7 and 8) and a slight dependence of n on T . However, as pointed out above

(see 'Response of the nucleation behaviour to a change in T_c '), a thermal history effect on n will be inevitable. Nevertheless, we observe that additivity is obeyed. It means that the slight temperature dependence of n will result in only a few additional nucleation sites at the lower temperature. Effectively, therefore, the Cahn condition is obeyed.

It should be noted that the additivity rule might not apply so easily for up-quench experiments. This is because the number of nuclei formed at a higher temperature following partial crystallization at a lower temperature will be characteristic of the lower temperature and independent of the higher temperature. This aspect of the work is currently being investigated.

CONCLUSIONS

The characteristics of the liquid-to-solid transformation behaviour of polyethylene have been described adequately in the literature, and our results corroborate the main observations, i.e. that:

(i) nucleation behaviour is pseudo-homogeneous with site saturation early in the process of crystallization;

(ii) crystal growth is initially linear, but slows down at later stages of crystallization;

(iii) morphology of the growing crystals changes from round, ringed spherulites, through coarse, non-ringed spherulites to axialites, with increasing temperature of crystallization; and

(iv) transformation isotherms can be superposed when plotted on a log (time) scale.

The results on additivity are limited to:

(i) the temperature range 121 to 129°C;

(ii) temperature step-down experiments; and

(iii) evaluations made at 50% transformation (i.e. not complete crystallization).

The results show that the additivity rule is obeyed for this system under the specified conditions.

ACKNOWLEDGEMENT

One of us (SC) acknowledges financial support from the

Australian Research Grants Scheme during the course of this work.

REFERENCES

- 1 Avrami, M. J. *Chem. Phys.* 1939, **7**, 1103
- 2 Avrami, M. J. *Chem. Phys.* 1940, **8**, 212
- 3 Cahn, J. W. *Acta Metall.* 1956, **4**, 572
- 4 Christian, J. W., 'The Theory of Transformations in Metals and Alloys', Pergamon, New York, 1965
- 5 MacFarlane, D. R. *J. Non-Cryst. Solids* 1982, **53**, 61
- 6 Ozawa, T. *Polymer* 1971, **12**, 150
- 7 Nakamura, K., Watanabe, T., Katayama, K. and Amano, T. *J. Appl. Polym. Sci.* 1972, **16**, 1077
- 8 Nakamura, K., Katayama, T. and Amano, T. *J. Appl. Polym. Sci.* 1973, **17**, 1031
- 9 Aggarwal, P. K. and Brimacombe, J. K. *Metall. Trans. (B)* 1981, **12**, 121
- 10 Hawbolt, E. B., Chau, B. and Brimacombe, J. K. *Metall. Trans. (A)* 1983, **14**, 1803
- 11 Cahn, J. W. and Hazel, W. C. in 'Decomposition of Austenite by Diffusional Processes' (Eds. Z. F. Zackay and H. I. Aaronson), Interscience, 1962
- 12 Kirkaldy, J. S., Uenugopalan, D. and McGirr, M., Proc. First National Heat Treatment Conference, Australian Inst. of Metals, 1984, pp. 1-12
- 13 Banks, W., Hay, J. N., Sharples, A. and Thomson, G. *Polymer* 1964, **5**, 163
- 14 Lanceley, H. A. *Polymer* 1965, **6**, 15
- 15 Hoffman, J. D., Frolen, L. J., Ross, G. S. and Lauritzen, J. I. *J. Res. NBS (A)* 1975, **79**, 671
- 16 Maxfield, J. and Mandelkern, L. *Macromolecules* 1977, **10**, 1141
- 17 Aggarwal, S. L., Markev, L., Kollar, W. L. and Geroch, R. *J. Polym. Sci. (A-2)* 1966, 715
- 18 Verhoeven, J. D., 'Fundamentals of Physical Metallurgy', Wiley, Chichester, 1975, p. 340
- 19 Chynoweth, K. R. and Stachurski, Z. H. *Polymer* 1986, **27**, 1912
- 20 Keith, H. D. and Padden, F. J., Jr. *J. Appl. Phys.* 1964, **35**, 1270
- 21 Keith, H. D. and Padden, F. J., Jr. *J. Appl. Phys.* 1964, **35**, 1286
- 22 Sharples, A. *Polymer* 1962, **3**, 250
- 23 Jain, N. L. and Swinton, F. L. *Eur. Polym. J.* 1967, **3**, 371
- 24 Chatterjee, A. M., Price, F. P. and Newman, S. J. *Polym. Sci. (A-2)* 1975, **13**, 2369
- 25 Cole, J. H. and St Pierre, L. E. *J. Polym. Sci., Polym. Symp.* 1978, **63**, 205
- 26 Hoffman, J. D. and Lauritzen, J. I. *J. Res. NBS (A)* 1961, **65**, 297
- 27 Barnes, W. J., Luetzel, W. G. and Price, F. P. *J. Phys. Chem.* 1961, **65**, 1742
- 28 Mandelkern, L. 'Growth and Perfection of Crystals', Wiley, New York, 1958
- 29 Mandelkern, L., Quinn, F. A., Jr and Flory, P. J. *J. Appl. Phys.* 1954, **25**, 830